CHAPTER 9

TRANSIENT PROPAGATION OF WAVES IN A FLUME

Kwok Fai Cheung[1], Michael Isaacson[2], Member ASCE, and Etienne Mansard[3]

ABSTRACT

A recently developed numerical method is applied to the study of transient, nonlinear wave propagation in a flume. The nonlinear free surface boundary conditions and the wave generator boundary condition are expanded about the corresponding equilibrium positions by perturbation expansions. The boundary conditions are then satisfied to second order by a numerical integration in time, and the field solution at each time step is obtained by an integral equation method based on Green's theorem. The propagation characteristics of regular, bichromatic and irregular waves are studied numerically, and the significance of nonlinear effects is highlighted.

1. INTRODUCTION

The numerical prediction of transient wave propagation in a flume has been the subject of investigation for a number of years. To a first approximation, linear wave theory may be used to describe the transient wave field. However, there are a number of shortcomings associated with this approach, which are mainly due to the neglect of higher order forced and free wave components. Although the amplitudes of these higher order components are generally small, these may become important for wave flume and basin tests involving wave interactions with harbours, floating breakwaters or moored vessels.

To account for nonlinear effects, the transient wave problem may be treated numerically by a time-stepping procedure, in which the full nonlinear free surface boundary conditions are applied on the instantaneous free surface and a new system of simultaneous equations is generated and solved at each time step as the free surface

[1] Design Engineer, Ports and Marine Department, Sandwell Inc., 1190 Hornby Street, Vancouver, B.C., Canada V6Z 2H6.

[2] Professor, Department of Civil Engineering, University of British Columbia, Vancouver, B.C., Canada V6T 1Z4.

[3] Senior Research Officer, Hydraulics Laboratory, National Research Council of Canada, Ottawa, Canada K1A 0R8.

moves to a new position (e.g. Longuet-Higgins and Cokelet, 1976; Kim et al., 1983; and Brorsen and Larsen, 1987). On the other hand, a second-order model defined on fixed boundaries can be obtained by the application of a perturbation expansion so that a solution to the system of simultaneous equations is required only once rather than at each time step. The boundary conditions to second order are then satisfied on the corresponding equilibrium positions by a numerical integration in time. Based on this approach, Isaacson and Cheung (1991, 1992) have treated the second-order diffraction problems in two and three dimensions respectively.

The theoretical treatment for the extension of the second-order diffraction method in two dimensions to include the effects of a moving wave generator has been described by Isaacson et al. (1993). The computed free surface elevations have been validated through comparisons with experimental results. The present paper summarizes the theoretical and numerical formulations of the method, and places emphasis on numerical results for the propagation of various transient wave trains and wave packets.

2. THEORETICAL FORMULATION

A description of the theoretical and numerical formulations has been given in detail by Isaacson et al. (1993) and only a brief outline of the method is given here. With reference to Fig. 1, the two-dimensional problem is defined with respect to a right-handed Cartesian coordinate system (x,z). The wave generator is located above a fixed vertical plate and extends from a distance h above the floor of the flume to the water surface. The generator may produce a combined piston/paddle motion defined by the generator's horizontal displacement δ at the still water level together with a rotation θ measured clockwise from the z axis. With the fluid assumed incompressible and inviscid, and the flow irrotational, the fluid motion is described by a velocity potential ϕ which satisfies the Laplace equation within the fluid domain and which is subject to boundary conditions on the generator surface S_W, the instantaneous free surface S_f at $z = \eta$, the flume floor $z = -d$, and a radiation surface S_C.

When the amplitude of the wave generator displacement is small compared to the height of the generator, and the water depth is not small compared with a typical wavelength, it is possible to apply Taylor series expansions to reduce the wave generator and free surface boundary conditions, originally derived on the instantaneous surfaces, to conditions evaluated at the corresponding equilibrium positions. The problem may then be defined with respect to a time-independent domain D which is bounded by the equilibrium generator surface S_g, the still water surface S_0, the flume floor and the control surface S_C. The first-order and second-order quantities in the formulation are further separated by introducing perturbation expansions for ϕ and η and taking the specified generator motion variables δ and θ to be first-order quantities:

$$\phi = \varepsilon \phi_1 + \varepsilon^2 \phi_2 + \cdots \tag{1}$$

$$\eta = \varepsilon \eta_1 + \varepsilon^2 \eta_2 + \cdots \tag{2}$$

$$\delta = \varepsilon \delta_1 \tag{3}$$

$$\theta = \varepsilon\theta_1 \tag{4}$$

where ε is a perturbation parameter related to the amplitude of the horizontal displacement of the wave generator which is small.

Substituting the power series representations for ϕ, η, δ and θ into the Laplace equation and the boundary conditions, including the expanded generator and free surface boundary conditions, separate boundary value problems may be developed for each of the ε and ε^2 terms in the power series. In the k-th order problem (k = 1, 2), the potential ϕ_k satisfies the Laplace equation

$$\nabla^2\phi_k = 0 \qquad \text{in D} \tag{5}$$

and is subject to the boundary conditions applied on the flume floor, the equilibrium generator surface and the still water surface. These are given respectively as

$$\frac{\partial\phi_k}{\partial z} = 0 \qquad \text{at } z = -d \tag{6}$$

$$\frac{\partial\phi_k}{\partial n} = f_k \qquad \text{on } S_g \tag{7}$$

$$\frac{\partial\phi_k}{\partial z} - \frac{\partial\eta_k}{\partial t} = f_k' \qquad \text{on } S_o \tag{8}$$

$$\frac{\partial\phi_k}{\partial t} + g\eta_k = f_k'' \qquad \text{on } S_o \tag{9}$$

Here t denotes time, g is the acceleration due to gravity and n is distance in the direction of the unit normal vector **n** directed outward from the fluid region. Each of the terms f_k, f_k' and f_k'' represents known expressions which can be evaluated from the specified motion of the wave generator and the solution at first order. In addition, the potential has to satisfy a radiation condition

$$\frac{\partial\phi_k}{\partial t} + c\frac{\partial\phi_k}{\partial n} = 0 \qquad \text{on } S_c \tag{10}$$

where c is the time-dependent celerity of the radiated waves on the control surface (see Orlanski, 1976; and Isaacson and Cheung, 1991). With the boundary conditions on each of the boundaries properly defined, the solution to the boundary-value problem is obtained by the application of a boundary integral equation involving a Green's function.

Initial conditions correspond to a stationary generator and still water in the computational domain. A wave train is subsequently generated by applying a prescribed time series for the generator motion. The generator boundary condition, the free surface boundary conditions and the radiation condition, which together govern the development of the flow, are satisfied by a numerical integration in time. Since the boundaries are invariant in time, the matrix equation obtained through a discretization

of the integral equation need be inverted only once rather than at each time step, with variations in time only affecting the input vector of the matrix equation. The maximum time-step size for a given discretization and excitation wave frequency can be determined by the Courant criterion, $c\Delta t/\Delta S \leq 1$, where Δt and ΔS denote respectively the time-step and facet sizes. This criterion has been tested numerically in the context of the second-order diffraction problem, and has been found to provide reasonable estimates (Isaacson and Cheung, 1991).

3. EXPERIMENTAL SET-UP AND PROCEDURE

In order to verify the present numerical model, a series of physical experiments were performed at the Hydraulics Laboratory of the National Research Council of Canada. The experiments were carried out in a flume of dimensions 1.2 x 1.2 x 67 m. A beach of uniform slope 1:25 was located at one end of the flume, and consisted of a sub-layer of coarse sand covered by a 10-cm layer of sharp stones (2-3 cm). Earlier measurements of wave reflection by the beach indicated that the reflection coefficient was below 5% over the wave frequency range 0.3 to 1.3 Hz. However, long waves with a frequency range 0.04 to 0.05 Hz encounter a relatively high degree of reflection, corresponding to reflection coefficients of the order of 40 to 50%.

The flume is equipped with a hydraulically driven wave generator which was operated in piston mode only. In the experiments described here, waves were generated in a water depth of 0.7 m and the free surface elevations at 12 diffcrent locations along the flume were monitored using twin wire capacitance wave probes. Data acquisition and analysis were performed using the Generalized Experiment control and Data Analysis Package (GEDAP; Miles and Funke, 1989) and the Real-Time Control (RTC) software packages (Crookshank, 1989). These allow all required probes to be sampled simultaneously. The sampling rate was chosen to be 0.05 sec, while the total sampling time for a typical test was chosen to be 100 sec.

4. RESULTS AND DISCUSSION

In the numerical and experimental results presented, a generator surface extending from the flume floor to the water surface has been adopted (i.e. $h = 0$ in Fig. 1) and the piston mode of the generator motion has been applied (i.e. $\theta = 0$). The computation was performed on an IBM 3090/150S computer at the University of British Columbia and double precision was used throughout. The variations of the free surface profiles in time and space are presented and the propagation characteristics of various transient wave trains are described. For the case of an irregular wave packet, simulated nonlinear free surface elevations at twelve different locations along the flume are compared with experimental results.

In the development of a regular or bichromatic wave train, there is a continuous influx of energy from the generator. In order to avoid an abrupt initial condition and allow a gradual development of the wave field, the periodic generator displacement is multiplied by a modulation function F_m such that the generator develops its motion gradually from zero to the prescribed amplitude over a specified modulation time T_m. For the case of regular wave diffraction to second order, testing by Isaacson and Cheung (1991) has indicated that, as a suitable choice, T_m may be taken to be equal to a typical wave period.

4.1 Regular Wave Train

Prior to an examination of results for irregular waves, the development and propagation of a regular wave train in time and space are first examined. For the case considered, the wave generator undergoes a sinusoidal displacement defined by $\delta(t) = \Delta \sin(\omega t) F_m$, where $\omega = 2\pi/T$ is the angular frequency, T is the wave period and Δ is the amplitude of the generator displacement. For a given wave frequency and water depth, the value of Δ can be related to the wave height by linear wave generation theory. Figs. 2 and 3 show the variations of the linear and nonlinear free surface profiles in space and time respectively. The incident wave conditions correspond to $kd = 2$ and $H/L = 0.08$, where k, H and L are respectively the wave number, the wave height and the wavelength of the resulting regular wave train. In the figures, $A = H/2$ is the wave amplitude. To ensure stability of the simulation, the facet and time-step sizes were taken respectively as $\Delta S = L/30$ and $\Delta t = T/60$, which correspond to a Courant number, $c\Delta t/\Delta S = 0.5$.

Fig. 2 shows linear and nonlinear free surface profiles along the flume at selected instants. At $t = 0$, the initial condition corresponds to still water everywhere in the computational domain. With the imposition of the generator motion over the first cycle, incident waves are gradually generated and propagate away from the generator at the corresponding group velocity. A steady state solution is developed near the generator after the first cycle, while the flow further from the generator takes somewhat longer to reach a steady state. It is noted that the initial waves of the wave train are unsteady with elongated lengths and smaller amplitudes, and appear to propagate at faster speeds. Without a radiation condition applied at the control surface, the reflection of these elongated initial waves would affect the flow near the test section well before a steady state solution has been developed.

Fig. 3 shows the time histories of the linear and nonlinear free surface elevations at four different locations along the length of the flume. For the location nearest to the wave generator, a stable steady-state solution for the free surface elevation is obtained for the entire period of simulation after a short duration of transient effects. Further down the flume, the duration of transient effects increases, and the initial waves are found to have longer periods as indicated above. It is also observed that a modulation is induced to the initial portion of the wave height envelope for the records at locations far away from the wave generator. At the last record, corresponding to a location 7 wavelengths away from the generator, a slight fluctuation of the free surface elevation is observed immediately after the modulation. These phenomena of wave front modulation and fluctuation have been examined analytically and similar results have been discussed by Mei (1983).

The numerical data also indicates that a system of second-order free waves at twice the incident frequency is also generated at the wave generator and propagates into the computational domain at the corresponding group velocity. These high frequency free waves are due to nonlinear interactions between the second-order free surface and the wave generator, and have also been observed in laboratory tests. Generally, the amplitude of these second-order free waves is small and does not have a significant effect on the overall wave profile. Since the numerical model is based on a second-order approach, the most obvious nonlinear effect in a regular wave train is to give rise to wave profiles with steeper crests and flatter troughs, whereas nonlinear effects on the celerity and group velocity are of higher order and cannot be reproduced here.

4.2 Bichromatic Wave Train

A bichromatic wave train at first order is composed of two primary harmonics propagating independently of each other, and each with a behaviour identical to a regular wave train. At second order, cross-interactions between the two harmonics give rise to a wave field which is modified to a greater extent.

Figs. 4 and 5 show the development of a bichromatic wave train in space and time respectively. The driving signal of the bichromatic wave train is obtained by adding a side-span harmonic signal to the excitation described in Section 4.1, such that the resulting signal is given by $\delta(t) = \Delta\,[\sin(\omega t) + \sin(0.8\omega t)]\,F_m$. Similar to the regular wave train, the bichromatic wave train develops its steady state solution rapidly. In Fig. 4, after a steady state solution has been developed, the same free surface profile repeats itself at an interval of 5T near the generator, which corresponds to the beat frequency of the signal. The free surface profile is also shown to repeat itself along the flume at a fixed interval. In Fig. 5, the time histories of the free surface elevation at selected locations along the flume are found to be virtually identical after an initial duration of a transient signal, which is greater for locations further along the flume.

Nonlinear effects associated with the super-harmonic interactions are indicated in Figs. 4 and 5 at locations where the amplitude of the free surface elevation is high, giving rise to steeper crests and flatter troughs than the linear theory predictions. However, a more careful inspection of the numerical results also indicates the presence of a second-order sub-harmonic component, which is phase-locked to the wave group structure, with troughs beneath the high waves and crests in between the wave groups. In addition, low-frequency spurious free waves which are generated nonlinearly through the second-order boundary conditions are also present in the numerical solution. Although the amplitudes of these second-order components are generally small, the correct reproduction of the second-order wave field is critical in the testing of systems with relatively low natural frequencies. Such considerations have given rise to research into the development of suitable second-order control signals (e.g. Barthel et al., 1983).

4.3 Regular Wave Packet

The examples studied so far represent a steady-state influx of energy at the wave generator. Despite a short duration of transient effects associated with the propagation of the initial waves, a steady-state solution near the wave generator can be developed rapidly in time and space. To further illustrate transient effects in wave propagation, the development a regular wave packet is considered here.

The modulation function applied to the regular and bichromatic wave trains is modified to incorporate a gradual decline from unity to zero during the fourth cycle. The regular wave packet is then generated by applying this modulation function to the regular wave signal described in section 4.1. Figs. 6 and 7 show the development of the regular wave packet in space and time respectively. In Fig. 7, immediate adjacent to the generator at $x/L = 1$, the amplitude of the wave packet is quite uniform and corresponds to that of a regular wave train. Further away from the generator, the amplitude of the packet increases slightly and then decreases gradually with time and distance away from the generator. The decrease in wave amplitude is associated with an increase in the length of the wave packet as the energy is dispersed to a greater extent.

Despite the changing wave amplitude, the period and wavelength in the core of the wave packet remain relatively constant. In addition to the elongated initial waves, a trail of short waves is also observed to lag behind the packet. Nonlinear effects associated with the superharmonics are more obviously observed, especially at locations of high waves. Due to the decrease in wave amplitude, nonlinear effects also decrease with distance away from the wave generator. On the other hand, the forced and free sub-harmonic components associated with the wave packet is not clearly observed here.

4.4 Irregular Wave Packet

To verify the present numerical procedure, the model has been applied to the simulation of a wave flume experiment performed at the Hydraulics Laboratory of the National Research Council of Canada. The experiment was carried out with a still water depth of 0.7 m. The generator was operated in piston mode and was used to generate an irregular wave packet by applying the generator displacement time history shown in Fig. 8. A spectral analysis of the displacement time history indicated two dominant peaks at 0.48 and 0.64 Hz. For the specified water depth of 0.7 m, these two frequency groups correspond to relative water depths kd = 0.92 and 1.32 respectively, and to celerities c = 2.30 and 2.12 m/s respectively. In the numerical model, the time-step and facet sizes were selected as 0.025 sec and 0.1 m respectively. On the basis of the Courant criterion, these values correspond to the capability of simulating celerities of up to about 4 m/s.

The measured and simulated nonlinear free surface elevations at twelve different locations along the flume are plotted as functions of time in Fig. 9. In general, comparisons between the numerical and experimental results indicate good agreement with respect to both the amplitude and phase, except for the portions of the records after the occurrence of the maximum amplitude. This may possibly be due to wave breaking that occurred near the generator in the experiment after the highest wave was generated. The discrepancies are first observed in the record corresponding to a location 4.11 m from the generator, with the simulated free surface elevation found to be higher than the measured elevation near time t = 25 sec. These differences appear to spread to a greater extent in the records for locations further down the flume. The discrepancies between the simulated and measured free surface elevations appear to be in the form of high frequency waves which travel at slower speeds, and appear to affect the later part of the records more significantly.

Even though the high and low frequency components in the applied displacement function are generated simultaneously, in the results presented the lower frequency components with higher amplitudes and celerities propagate ahead of the higher frequency components, so that the randomness of the wave profiles as shown in Fig. 9 appears to decrease with time. Although the frequency content of the entire record (100 seconds long) measured at various locations along the flume remains basically the same, the time-histories of the free surface elevations at different locations as shown in Fig. 9 are modified more significantly. Since components of similar frequencies propagate at approximately the same speed, after a long duration of simulation the free surface profile and elevation are characterized by a series of beat phenomena with successive frequencies and amplitudes. The overall decline in wave amplitude with distance from the generator is partly attributed to the segregation of the different frequency components and partly to the amplitude dispersion of a wave packet as discussed in section 4.3.

In addition to predicting the linear and nonlinear wave fields, the present numerical model provides a useful alternative approach in the study and analysis of the various transient, nonlinear wave phenomena. A potential application of the method is to the calculation of suitable first and second-order generator control signals which may be required prior to carrying out particular flume tests.

5. CONCLUSIONS

A time-domain second-order method for the simulation of transient, nonlinear wave propagation in a flume is summarized. The boundary conditions are satisfied to second order by a time-stepping procedure, and the field solution at each time step is obtained by an integral equation method based on Green's theorem. Since the boundaries are invariant in time, the solution to the matrix equation obtained through a discretization of the integral equation is required only once and can be applied to different time histories of generator motion. The method is applied to a study of the transient propagation of various wave trains and wave packets.

Free surface profiles along the flume and time histories of the free surface elevation are obtained for a regular wave train, a bichromatic wave train, and regular and irregular wave packets. For the case of a regular wave train, the numerical model is shown to be stable and robust, and is capable of maintaining a steady state condition for a sufficiently long duration of simulation. The propagation of a bichromatic wave train is similar to that of a regular wave train, but includes an additional second-order sub-harmonic component. The propagation of the regular and irregular wave packets is found to be unsteady and transient, given its varying wave profile along the length of the flume. For the case of an irregular wave packet, time histories of the water surface elevation along a wave flume are compared with those predicted by the numerical model and these indicate favourable agreement. Second-order effects in transient wave propagation have been highlighted and potential applications of the second-order wave model are indicated.

REFERENCES

Barthel, V., Mansard, E.P.D, Sand, S.E. and Vis, F.C. 1983. Group bounded long waves in physical models. *Ocean Engrg.*, 10(4), 261-294.

Brorsen, M. and Larsen, J. 1987. Source generation of nonlinear gravity waves with the boundary integral equation method. *Coastal Engrg.*, 11, 93-113.

Crookshank, N.L. 1989. Experimental control and data acquisition systems at the Hydraulics Laboratory of the National Research Council of Canada. *Proc. Workshop on Instrumentation for Hydraulic Laboratories*, Burlington, Ontario, pp. 92-110.

Isaacson, M., and Cheung, K.F. 1991. Second-order wave diffraction around two-dimensional bodies by time-domain method. *Appl. Ocean Res.*, 13(4), 175-186.

Isaacson, M. and Cheung, K.F. 1992. Second-order wave diffraction in three dimensions. *J. Waterway, Port, Coastal and Ocean Engrg.*, ASCE, 118(5), 496-516.

Isaacson, M., Cheung, K.F., Mansard, E. and Miles, M.D. 1993. Transient wave propagation in a laboratory flume. *J. Hydraulic Res.*, in press.

Kim, S.K., Liu, P.L.-F. and Liggett, J.A. 1983. Boundary integral equation solutions for solitary wave generation, propagation and runup. *Coastal Engrg.*, 7, 299-317.

Longuet-Higgins, M. and Cokelet, E.D. 1976. The deformation of steep surface waves on water. I. A numerical method of computation. *Proc. Royal Society London*, Ser. A, 350, 1-25.

Mei, C.C. 1983. *The Applied Dynamics of Ocean Surface Waves*. John Wiley and Sons, N.Y., 740 pp.

Miles, M.D. and Funke, E.R. 1989. The GEDAP software package for Hydraulics Laboratory data analysis. *Proc. Workshop on Instrumentation for Hydraulic Laboratories*, Burlington, Ontario, pp. 45-66.

Orlanski, I. 1976. A simple boundary condition for unbounded hyperbolic flows. *J. Comp. Physics*, 21, 251-269.

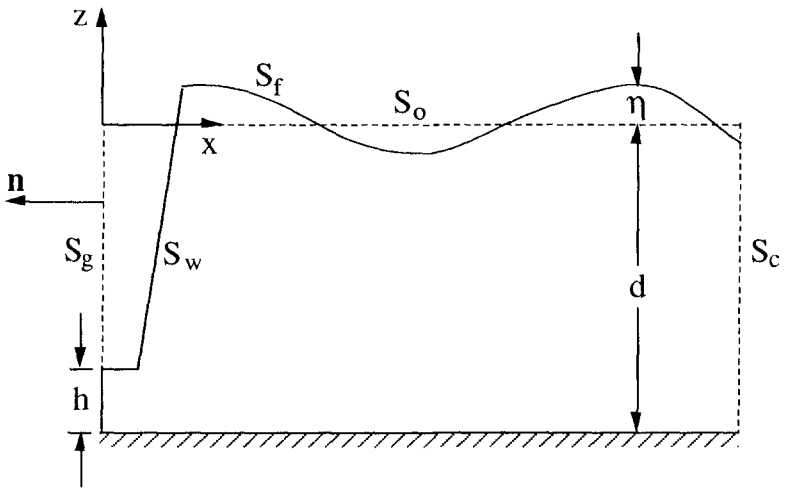

Fig. 1. Definition sketch of mathematical model.

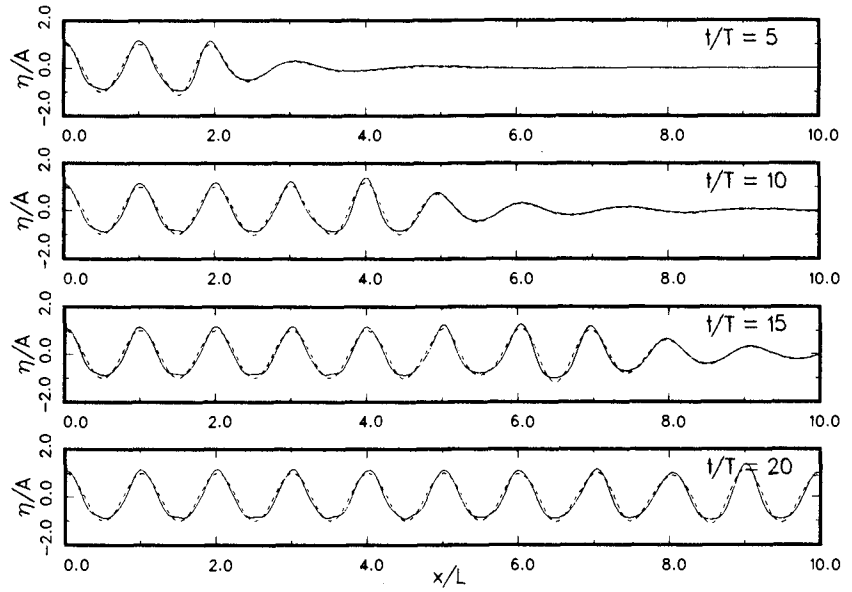

Fig. 2. Free surface profiles along the wave flume at various instants for a regular wave train. - - - -, linear solution; ——, nonlinear solution.

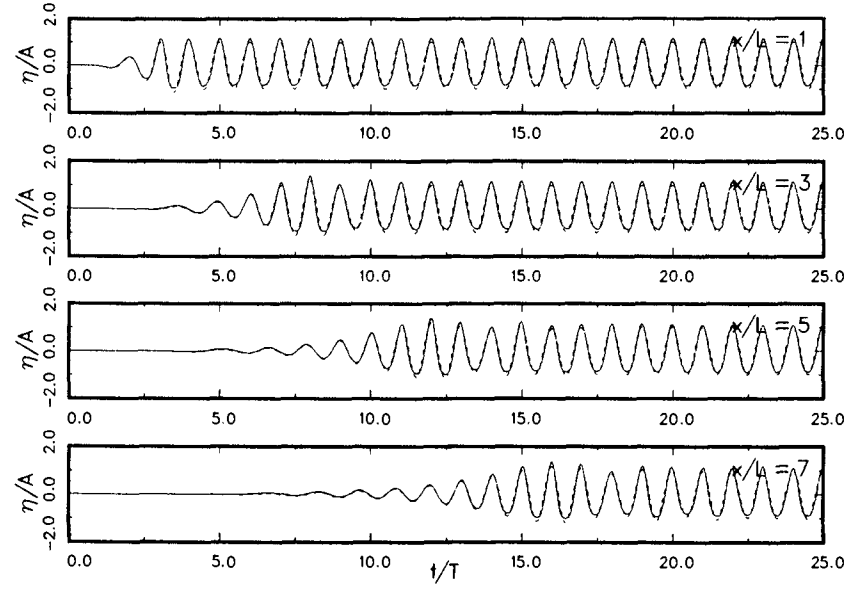

Fig. 3. Time histories of free surface elevation at various locations along the flume for a regular wave train. - - - -, linear solution; ——, nonlinear solution.

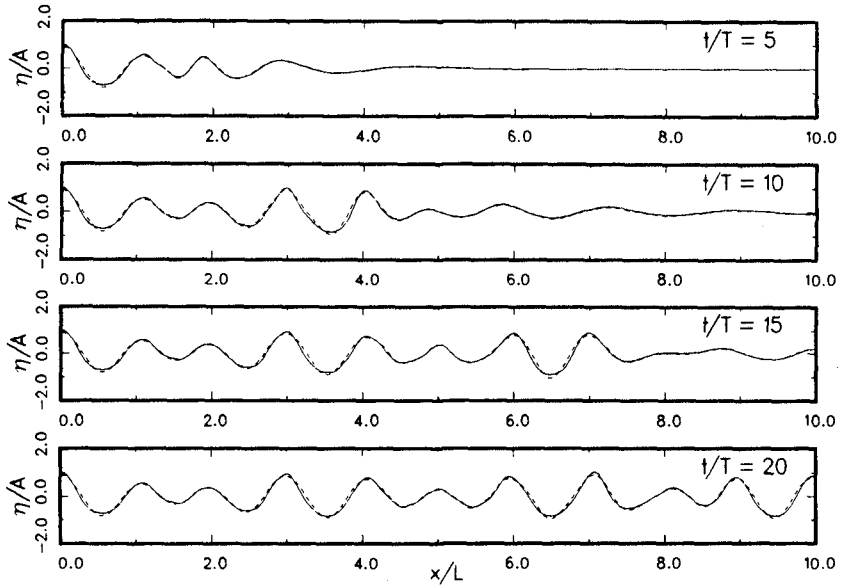

Fig. 4. Free surface profiles along the wave flume at various instants for a bichromatic wave train. - - - -, linear solution; ——, nonlinear solution.

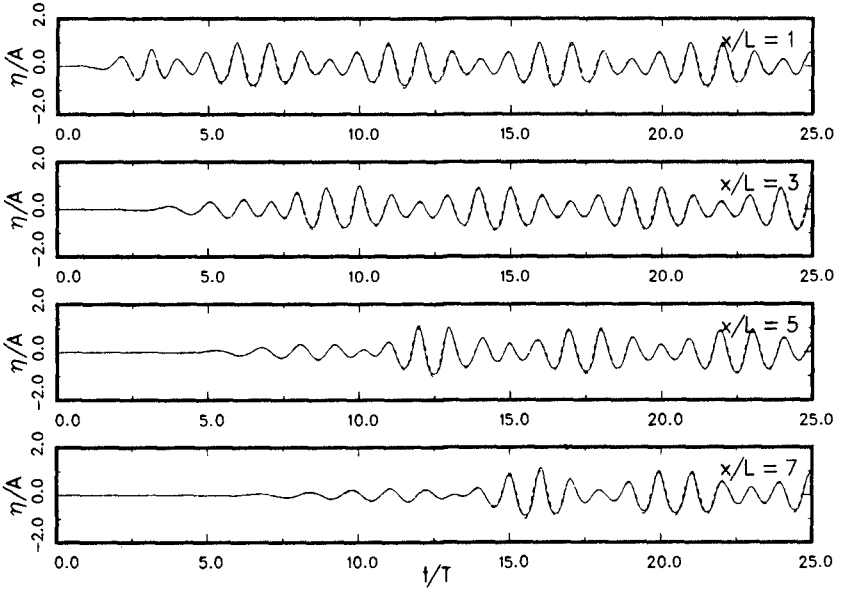

Fig. 5. Time histories of free surface elevation at various locations along the flume for a bichromatic wave train. - - - -, linear solution; ——, nonlinear solution.

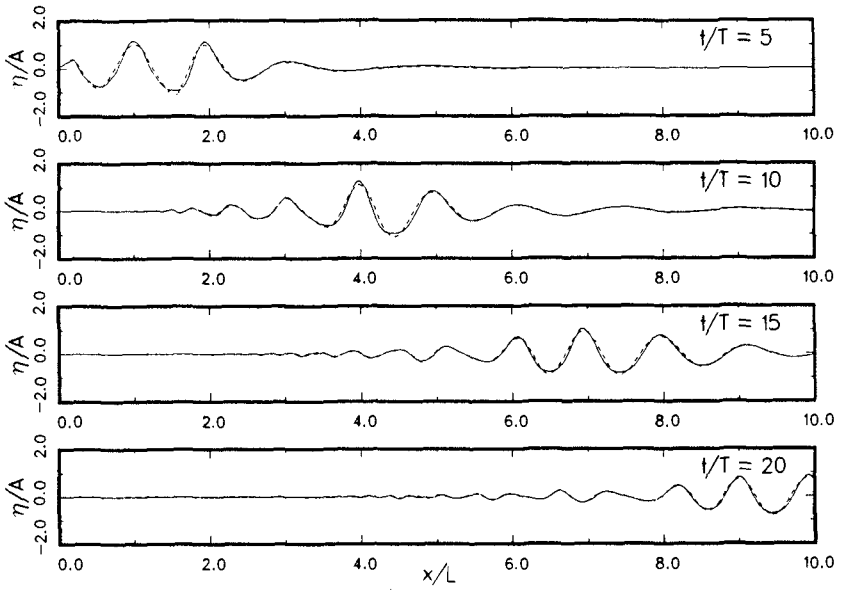

Fig. 6. Free surface profiles along the wave flume at various instants for a regular wave packet. - - - -, linear solution; ——, nonlinear solution.

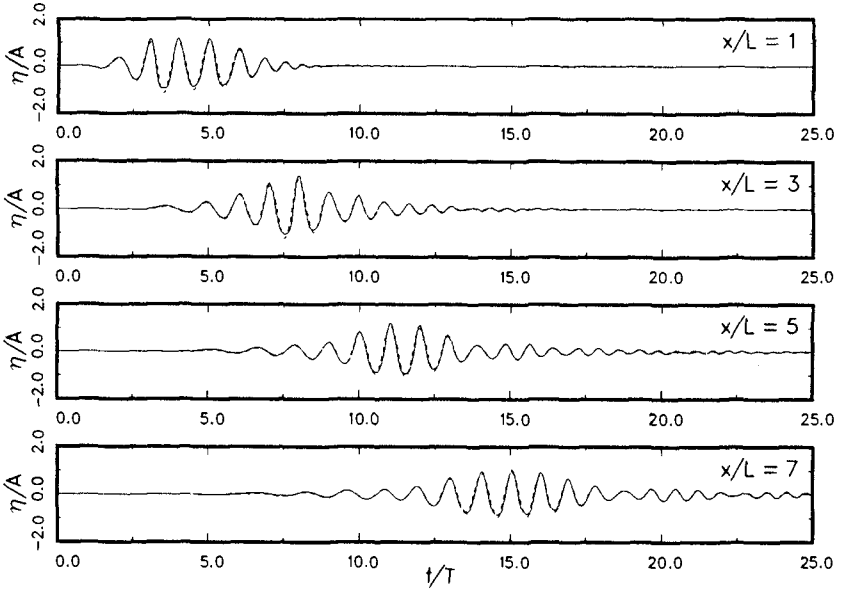

Fig. 7. Time histories of free surface elevation at various locations along the flume for a regular wave packet. - - - -, linear solution; ——, nonlinear solution.

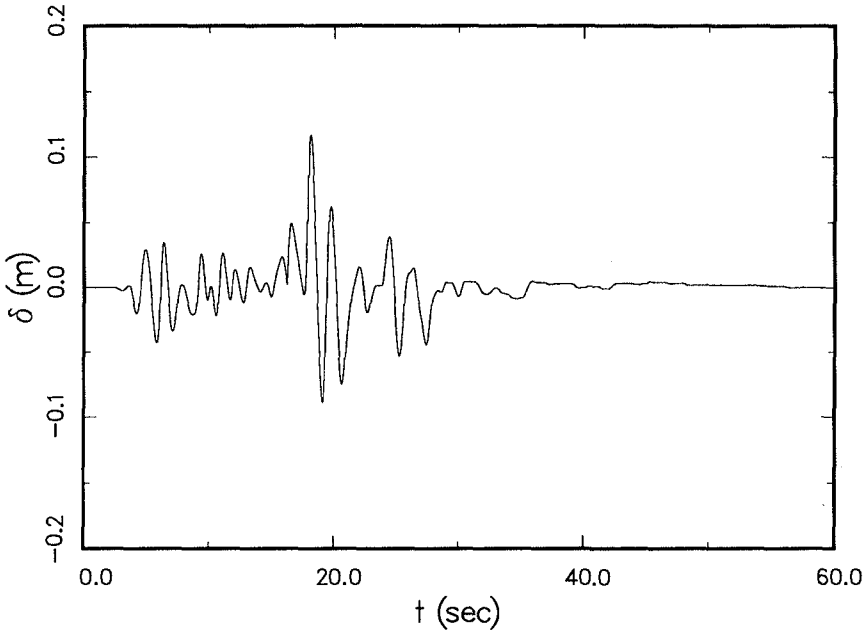

Fig. 8. Time history of wave generator displacement (piston mode) for an irregular wave packet.

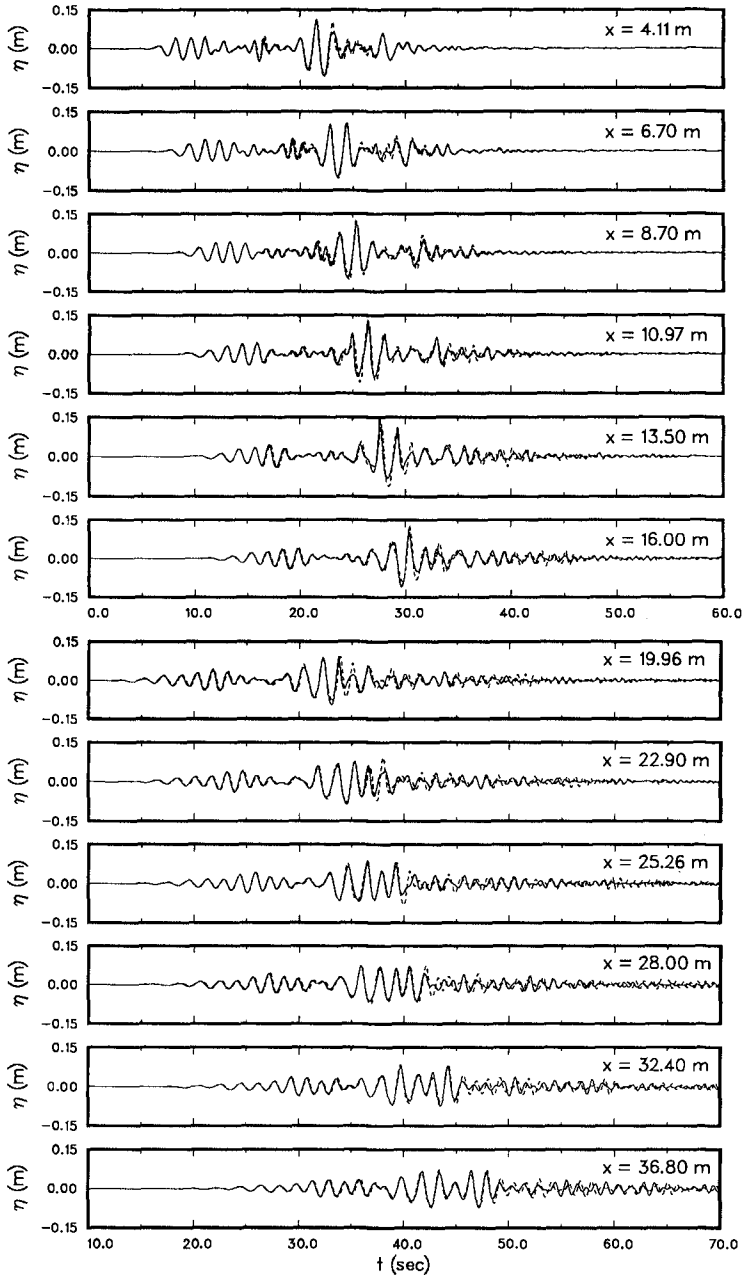

Fig. 9. Time histories of free surface elevation at various locations along the flume for an irregular wave packet. - - - -, simulated; ———, measured.